Multi-Terrains Assistive Force Parameter Optimization Method for Soft Exoskeleton

Lei Sun, *Member, IEEE*, Jiahui Jing, Chenghui Li, and Rundong Lu

***Abstract*— Due to the complexity of terrain in natural environments, the soft exoskeleton cannot adaptively adjust parameters to achieve the optimal performance. To this end, a design for a soft exoskeleton assistive force parameter optimization method on multi-terrains is presented in this paper. Firstly, the core control parameters are determined by analyzing the system's motion dynamics. Then, the collected data from inertial measurement unit (IMU) is transferred to the convolutional neural network (CNN) to recognize the certain terrain. In the meanwhile, the control parameters corresponding to the different terrains are optimized by the Bayesian algorithm. Finally, the optimal assistive force parameters are transferred to the system for improving the performance of the soft exoskeleton. The experiment is conducted on three participants, wherein the net metabolic rates of the subjects are compared with and without the assistive force. The final results show that the metabolic rates of the subjects reduce the average value of 19.6% on flat ground, 11.6% on walking uphill, and 12.7% on walking upstairs. The experimental results confirm the effectiveness of the proposed method.**

***Index Terms*— Bayesian optimization, soft exoskeleton, multiple terrains recognition, assistive force.**

I. Introduction

THE robotic exoskeleton is a newly developing auxiliary tool for assistance with human movement. It integrates the operator with the electromechanical equipment to improve the walking ability and weight-bearing capacity. This technology has broad application prospects in the field of rehabilitation training [1]. According to structural differences, lower limb exoskeletons can be categorized as rigid exoskeletons and soft exoskeletons. The rigid exoskeleton can provide more assistive torque, with more powerful machinery that boosts the wearer's load-bearing capacity. However, it also tends to have poor flexibility, and thus limits the bodily activities of the operator [2]. The soft exoskeleton is constructed with more flexible materials, such as Bowden cable. It is more lightweight and flexible than the rigid exoskeleton and thus has important research significance and social value [3], [4], [5].

By combining its own mechanical structure, control system and human-computer interaction, the soft exoskeleton achieves assistive force for the wearer on the basis of its own protection and motion intent recognition [6], [7], [8]. In the past five years, soft exoskeletons have made breakthroughs in various fields such as the assistive mode, motion intent recognition and adaptive control algorithm. Ulkir et al. [9]. proposed a data-driven predictive control (DDPC) algorithm. Their experiment verified that DDPC outperforms the PID controller in trajectory tracking with different conditions. Ma et al [10] proposed an underactuated soft exoskeleton by using a single motor to assist knee extension and ankle plantarflexion. The experimental results show that the exoskeleton device is helpful to produce sequential assistive force at each joint effectively. A new controller based on parametric optimal iterative learning control (POILC) was proposed by Chen et al [11]. The controller selected different auxiliary strategies for different terrains and reduce tracking errors. Liu et al. [12] proposed a man-machine cooperative control method based on the analysis of surface Electromyogram(EMG) signals. With the surface EMG signal and joint angle, regression analysis was used to predict the value of joint torque. Zhang et al. [13] proposed a control framework based on model-free reinforcement learning (RL) to optimize the control parameters. With consideration on this operation, the exoskeleton provided personalized assistive torque curves in order to achieve hip assistive force during walking.

The Bayesian Optimization algorithm can search the appropriate parameters automatically for obtaining optimal performance through a finite number of trials. It is also often used in the parameter optimization of exoskeleton robots. Gordon et al. [14] proposed a method for identifying the location of an ideal exoskeletal cuff with the human-in-the-loop optimization process. It used a Bayesian optimization algorithm to determine the optimal position of the exoskeletal cuff by measuring the subject's muscle activity. A sample-efficient method was proposed to adopt a model-based walking controller for a lower-limb exoskeleton based on Bayesian Optimization [15]. The effectiveness of the proposed method was finally demonstrated experimentally.

The terrain where people walk is often different. In different terrains, the control parameters should be matched accordingly. Therefore, in this paper, the Bayesian

Manuscript received 5 December 2022; revised 27 March 2023; accepted 7 April 2023. Date of publication 13 April 2023; date of current version 19 April 2023. This work was supported by the National Natural Science Foundation of China under Grant 62103300. *(Corresponding author: Jiahui Jing.)*

This work involved human subjects or animals in its research. Approval of all ethical and experimental procedures and protocols was granted by the Biomedical Ethics Committee, Tianjin University of Technology, Tianjin, China.

The authors are with the School of Electrical Engineering and Automation, Tianjin Key Laboratory for Control Theory and Applications in Complicated Systems, Tianjin University of Technology, Tianjin 300384, China (e-mail: sunleiftd@126.com; jjh157550@126.com; lch2488196746@126.com; 1183920333@qq.com).

Digital Object Identifier 10.1109/TNSRE.2023.3267062

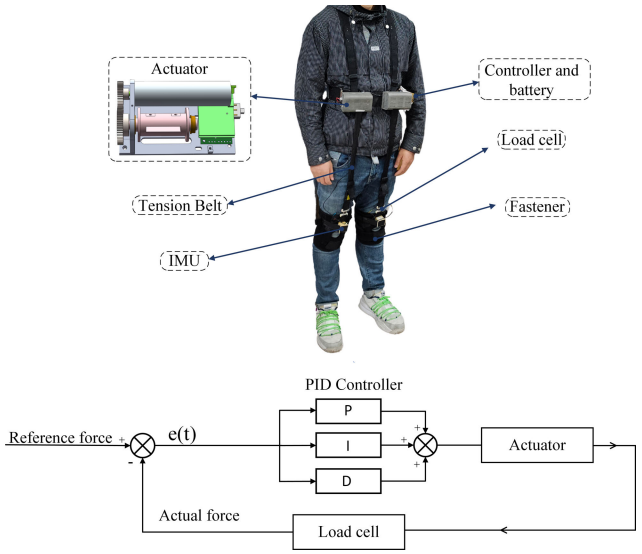

Fig. 1. The soft exoskeleton for hip assistive force and flow diagram of PID.

optimization algorithm is selected to solve the multi-terrains adaptive optimization problem of soft exoskeleton. The proposed method has three major contributions as follows:

1) The assistive force parameters are determined by analyzing the system's motion dynamics. The terrains are recognized by the CNN model.

2) The assistive force parameters corresponding to the certain terrain are optimized by the Bayesian algorithm.

3) The optimal assistive force parameters are transferred to the system for improving the performance of the soft exoskeleton. The final results show that on the net metabolic rate decreased by 12.7% (up stairs), 11.6% (uphill), and 19.6% (flat ground) averagely.

II. The Proposed Methods

A. Hardware Structure

Our exoskeleton device consists of six main parts: controller, actuator module, tension band, tension sensor, inertial sensor, and battery. The soft exoskeleton is shown in Fig.1 STM32F429 chip has been selected as the primary controller. The actuator mainly consists of the motor, motor driver, gear, and reel. One end of the strap is attached to the reel, the other end is connected to the fixation device on the knee. The IMU sensor is fixed under the knee to collect the hip joint swing's angle and angular velocity. The tension sensor is connected to the tension band at one end, the other end is connected to the knee fixation device, which is used to collect the interactive force. The master control collects changes in the angle and angular velocity of the hip joint during the wearer's walk to determine the assistive time and the assistive force. Meanwhile, the reference force value is derived from the assistive force equation. A force closed-loop method for controlling the device is selected to transfer the assistive force to the wearer. The error between the actual force and the reference force is used as the input to the PID control algorithm. The reference force is calculated by the assistive function which will be introduced in chart B. With the PID algorithm, the actual force tends to be the reference force.

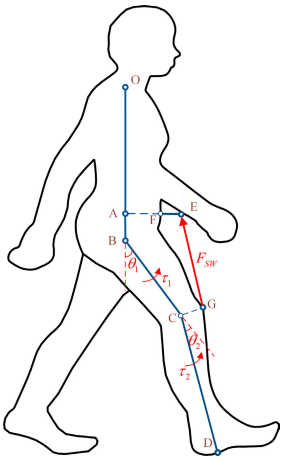

Fig. 2. Human dynamic model.

B. System Dynamics

In this section, the parameters influence on the soft exoskeleton are given by the analysis of the motion dynamics. The Lagrangian energy method is utilized to establish the dynamics equations for the human-machine system with the soft exoskeleton in the sagittal plane [16]. The human dynamics model is shown in Fig. 2. O is the human head. B is the human hip joint. C is the knee joint. D is the human simplified foot. E is the force point of the exoskeleton drive device. F is the fixed point of the waist of the exoskeleton device. OB is the upper limb torso. Its weight and length can be defined as m_0 and L_0 respectively. BC is the thigh. Its weight, rotational inertia, and length are defined as m_1, J_1, and L_1 respectively. CD is the lower leg. Its weight, inertia of rotation, and length are given by m_2, J_2 and L_2. The exoskeleton device is defined as the weight of m_E. F_{SW} is the exoskeleton assistive force value. Assume that the torso is vertical and the velocity $\vec{V} = (X, 0)$ in the sagittal coordinate system is uniform. Define the coordinate origin as the hip joint B, and the positive direction of x-axis as the walking direction.

According to the dynamics model, the position vectors $\vec{r}_1$ and $\vec{r}_2$ defined as follows:

$$\vec{r}_1 = \overrightarrow{BC} = [L_1 \sin\theta_1 \ -L_1 \cos\theta_1]^T, \tag{1}$$

$$\vec{r}_2 = \overrightarrow{BD} = [L_1 \sin\theta_1 + L_2 \sin\theta_2 - L_1 \cos\theta_1 \\ -L_2 \cos(\theta_1 - \theta_2)]^T, \tag{2}$$

where θ_1 and θ_2 are the hip and knee flexion angles.

The kinetic energy of the system T_{SW} is defined as:

$$\begin{aligned} T_{SW} &= T_{OB} + T_{BC} + T_{CD} + T_{EF} \\ &= \frac{1}{2} m_0 \vec{V}^2 + \frac{1}{2} m_1 \vec{V}^2 + \frac{1}{2} J_1 \omega_1^2 \\ &\quad + \frac{1}{2} m_2 \left(\frac{d\vec{r}_1}{dt} \right)^2 + \frac{1}{2} J_2 \omega_2^2 + \frac{1}{2} m_E \vec{V}^2. \end{aligned} \tag{3}$$

The total potential energy P_{SW} is given by:

$$\begin{aligned} P_{SW} &= P_{OB} + P_{BC} + P_{CD} + P_{EF} \\ &= \left(-\frac{1}{2} m_1 - m_2 \right) g L_1 \cos\theta_1 - \frac{1}{2} m_2 g L_2 \cos(\theta_1 - \theta_2) \\ &\quad + \frac{1}{2} m_0 g L_0 + m_E g b. \end{aligned} \tag{4}$$

The Lagrangian operator L_{SW} can be calculated as:

$$L_{SW} = T_{SW} - P_{SW}. \tag{5}$$

The Lagrangian equation is calculated by combining equations (3), (4), and (5). Its term is defined as:

$$\frac{d}{dt}\begin{bmatrix} \frac{\partial L_{SW}}{\partial \dot{\theta}_1} \\ \frac{\partial L_{SW}}{\partial \dot{\theta}_2} \end{bmatrix} - \begin{bmatrix} \frac{\partial L_{SW}}{\partial \theta_1} \\ \frac{\partial L_{SW}}{\partial \theta_2} \end{bmatrix} = \begin{bmatrix} \tau_1 + \tau_2 + \tau_{SW} \\ \tau_2 \end{bmatrix}. \tag{6}$$

where τ_{sw} is the exoskeleton's assistive torque to the hip joint, τ_1 and τ_2 are the equivalent muscle torque of the hip and knee joints. The dynamics equations of the man-machine system are given as follows:

$$M(\theta)\ddot{\theta} + G(\theta) = \tau + \tau_a, \tag{7}$$

In the equation (7), the specific expressions for each term are given as follows:

$$\begin{aligned} \tau &= [\tau_1 + \tau_2]^T \\ \tau_a &= [\tau_{SW} 0]^T \\ \ddot{\theta} &= \begin{bmatrix} \ddot{\theta}_1 & \ddot{\theta}_2 \end{bmatrix} \\ M(\theta) &= \begin{bmatrix} \frac{1}{3}\left(m_1 L_1^2 + 4m_2 L_2^2\right) & -\frac{1}{3}m_2 L_2^2 \\ -\frac{1}{3}m_2 L_2^2 & \frac{1}{3}m_2 L_2^2 \end{bmatrix} \\ G(\theta) &= \begin{bmatrix} \frac{1}{2}(m_1 + 2m_2) g L_1 \sin\theta_1 + \frac{1}{2}m_2 g L_2 \sin(\theta_1 - \theta_2) \\ -\frac{1}{2}m_2 g L_2 \sin(\theta_1 - \theta_2) \end{bmatrix}, \end{aligned} \tag{8}$$

According to the dynamics equation (7), the human motion track can be affected by the torque $\tau + \tau_a$. In the condition of the same track, the torque $\tau + \tau_a$ is fixed curve. The change of the assistive torque τ_a can directly affect the joint torque τ of the human body. The assistive torque τ_a is tuned by the assistive force function. In this paper, we use the assistive force function to determine the soft exoskeleton assistive force value [17]. The terms of the assistive force function are given as follows:

$$F(t) = A\sin(\pi\frac{t}{T} + \alpha\sin(\pi\frac{t}{T})) + f, \tag{9}$$

where F represents the output assistive force. f represents the preload force (usually set to constant). t represents the timing of the assistive force. T is the period value of the swing phase. In this paper, we take the average time of the first three swing phases as the T. α is a phase shift factor. A represents the assistive force amplitude.

The effect of the assistive force amplitude A and the phase shift factor α with different parameters is shown in Fig.3(a) and Fig.3(b). The swing phase amplitude A determines the peak magnitude of the function waveform. Different shift parameters α affect the peak position of the assist force curve. Different assist force curves will produce different assistive torque. Different assistive torques on the hip joint will have different assistive effects. Therefore, the parameters α and A are selected as optimization parameters.

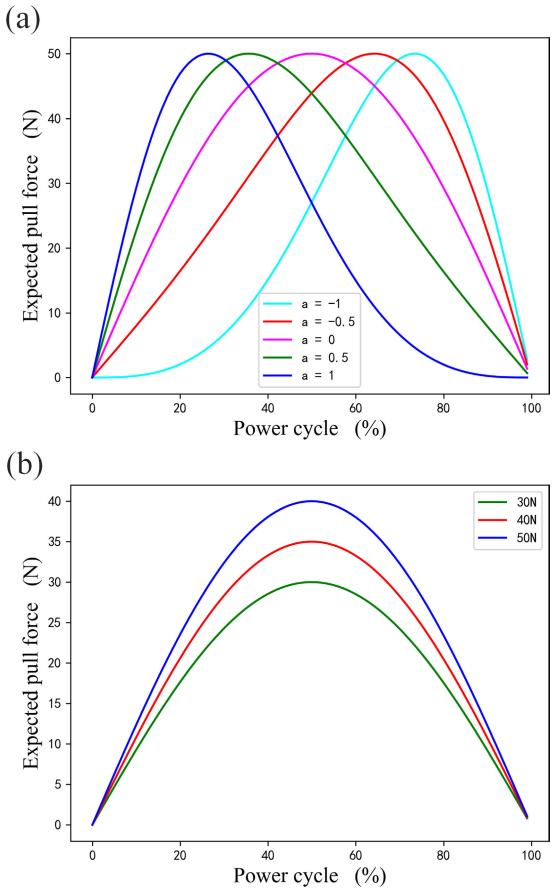

Fig. 3. The curves of the assistive force function on different parameters.

C. Bayesian Optimization Algorithm

The Bayesian optimization algorithm is a method for calculating the global extrema of an unknown objective function by learning the shape of the objective function and finding the parameters that make the objective function approach the global optimum [18]. The Bayesian optimization algorithm consists of a probabilistic surrogate model and an acquisition function. The probabilistic surrogate model includes a prior probability model and an observation model. The probabilistic surrogate model can estimate the distribution of the unknown objective function based on a finite number of observations. An acquisition function is constructed from the posterior probability distribution and used to determine the next observation [19]. A functional relationship between the parameters to be optimized and the objective function as follows:

$$x^* = \arg_{x\in X}\max\left(f(x)\right). \tag{10}$$

In this paper, x denotes the parameters A and α to be optimized. $f(x)$ is an unknown objective function with the mapping relationship between the optimized parameters (A, α) and the D-value of the heart rate variation.

The Gaussian process is selected as the probabilistic surrogate model. Gaussian process can obtain the function distribution by using the sampling point (x, y), where x is the assistive force parameters to be optimized. y is the D-value of the heart rate variation(quiescent condition and walking state) on different parameters [19], [20]. The D-value on heart rate

variation is sensitive to the state of the human body in different terrains with different parameters.

The Gaussian process is an extension of a multivariate Gaussian distribution to infinite dimensions, including the mean function and covariance function [21]. The formulae is as follows:

$$f(x) \sim GP\left(\mu(x), K\left(x, x'\right)\right), \tag{11}$$

where $\mu(x)$ is the mean function and $K\left(x, x'\right)$ is the covariance function. Typically, the mean can be set to zero. The covariance function always uses a Gaussian kernel function, which will be modified and expressed as follows:

$$K\left(x, x'\right) = \sigma_f^2 \exp\left[-\frac{\left(x - x'\right)^2}{2l^2}\right] + \sigma_n^2 \delta\left(x, x'\right), \tag{12}$$

where $\delta\left(x, x'\right) = \begin{cases} 1 & \text{x=x}' \\ 0 & \text{x} \neq \text{x}' \end{cases}$, $\sigma_n = 3$, σ_f and l are hyperparameters. After that, we can determine the expression for the prediction point based on the posterior probability as follows:

$$\begin{bmatrix} y \\ y_* \end{bmatrix} \sim N\left(0, \begin{bmatrix} K & K_*^T \\ K_* & K_{**} \end{bmatrix}\right). \tag{13}$$

With the Gaussian regression process, the function distribution on heart D-value can be obtained by the sampling points. The acquisition function will generate the new sampling points. In this paper, Upper Confidence Bound(UCB) is used as a Bayesian optimal acquisition function [22].

$$UCB = \mu(x) + k\sigma(x) \text{ k} \geq 0. \tag{14}$$

In the equation (14), $\mu(x)$ denotes the mean of the sampling points. $\sigma(x)$ denotes the variance of the sampling points. The x corresponding to the largest UCB is selected as the next sampling point.

D. Heart Rate Data Acquisition

Heart rate is a common metric for characterizing the state of the human body. It is sensitive to the state change of the human movement. Therefore, in this paper, the heart rate data is collected as a reference quantity for evaluating the state of human movement. The objective of our Bayesian optimization algorithm is to obtain the parameters A and α corresponding to the smallest heart rate variation under different terrains.

In order to obtain human exercise data, we chose a heart rate band as the data collector. In addition, the phase shift parameter α was set in the range of [-1,1] and A was set the range of [30, 50]. We finally selected [−1, 50],[−0.5, 50],[−0.5, 40],[−1, 40],[−0.5, 30],[1, 40],[0.5, 45],[−1, 35],[0, 35],[1, 50] and [0, 50] as our acquisition values. On this basis, six volunteers were recruited for data collection. All volunteers signed an informed consent form before the start of the experiment. The details of volunteers A to F are shown in Table I.

For the staircase exercise, a real staircase was chosen as the data collection environment. For the other two exercise modes, a treadmill with a normal speed of 4 km/h was chosen for data collection. In the experiment, six volunteers wore exoskeletons and heart rate bands. The real-time heart rate was collected via a mobile phone app. Before the formal experiment began, the volunteers measured each individual's normal heart rate without the exoskeleton, as each individual's physical and environmental factors could affect the results. Each subject then wore the exoskeleton and sat down for a period of time with the heart rate monitor turned on. After observing the subjects' heart rate data return to relaxed state, each subject began a 5-minute static heart rate measurement, followed by the start of formal data collection for the three terrains.

TABLE I
TESTER DATA

Tester	sex	age	High(cm)	Weight(kg)
Tester A	man	25	182	76
Tester B	man	27	175	64
Tester C	man	25	185	75
Tester D	man	24	173	70
Tester E	man	24	170	75
Tester F	man	26	169	65

Fig. 4. The D-value on heart rate were collected on flat ground, on the stair, and ramp.

For the assistive parameters corresponding to upstairs terrain, volunteers wearing the exoskeleton with a heart rate band were asked to walk up and down a seven-story staircase twice before the collection of heart rate data. After a ten-minute rest period at the starting point, the volunteers continued the staircase test with other sets of assistive force parameters until all six volunteers and 11 sets of assistive force parameters had been tested. The final D-value between the volunteer's mean heart rate in the initial resting state and the mean heart rate after exercise was considered as the change in heart rate corresponding to the selected parameters. The heart rate dataset was composed by the D-values corresponding to the different parameters.

The experimental procedure for heart rate acquisition on flat terrain and walking uphill was the same as that for walking up stairs, and the data acquisition process is shown in Fig.4. The final heart rate data corresponding to 11 sets of assistive force parameters were obtained for the three terrains and this was used as the data set for Bayesian optimization of the parameters.

E. Parameter Optimization

The average D-value on heart rate changes with different parameters was collected under three assistive exercises, namely walking upstairs, walking uphill and walking on flat ground. Next, these data were used as the input data of the Bayesian optimization algorithm to finally get the optimal solution.

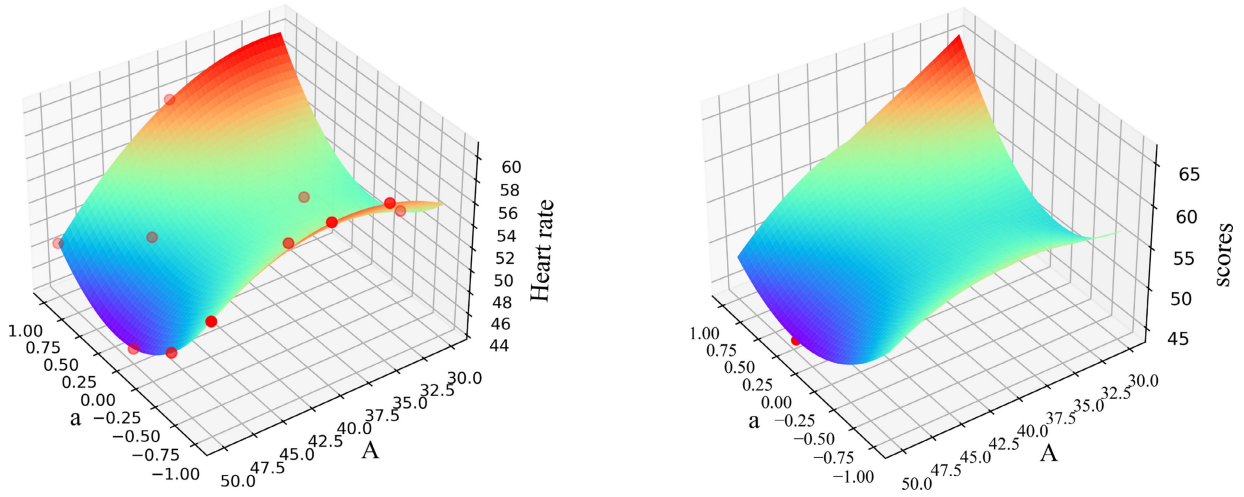

Fig. 5. Parameter optimization results of the walking upstairs mode.

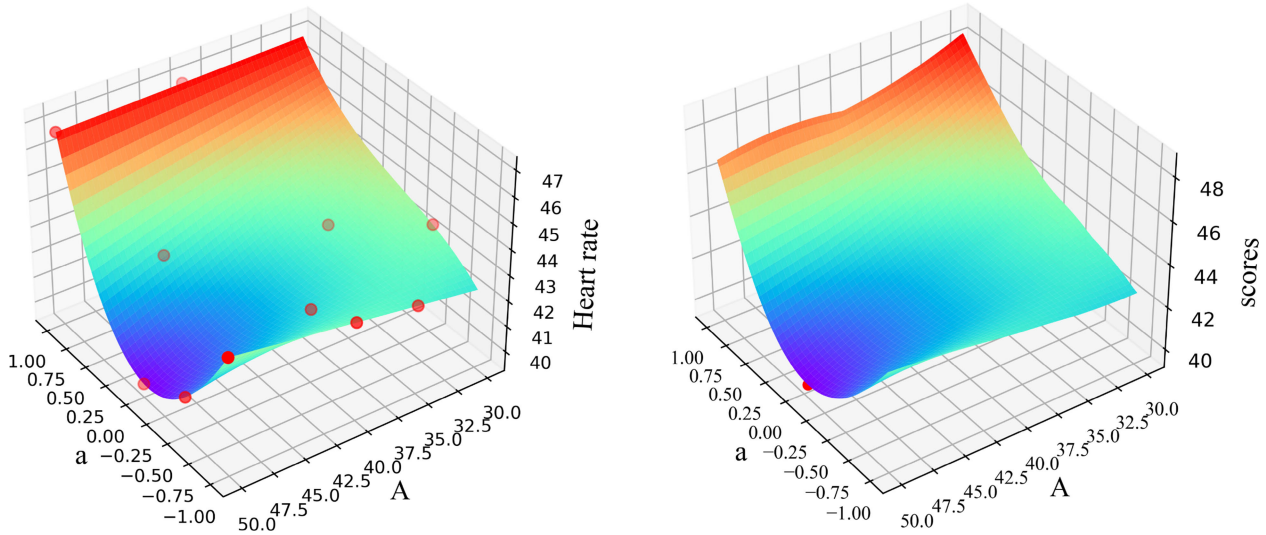

Fig. 6. Parameter optimization results of the walking uphill mode.

Firstly, Bayesian iterative optimization was performed on the data collected from the stair walking. The total number of iterations was set at 10 in the optimization algorithm, and the exploration parameter was e = 0.2. The optimized parameters and the corresponding heart dataset were sent to the Bayesian optimizer to obtain the optimal solution after three iterations. The optimization results are shown in Fig.5. The left side corresponds to the objective function, and the right side corresponds to the acquisition function. As can be seen from the table, with the increment of the value A, when walking upstairs, the exoskeleton operator showed a more natural heart rate decline. The dynamical parameters of the α change of heart rate variation also had a certain influence. Finally, it was concluded that the optimal parameters are $A = 50$ and $\alpha = 0.212$. The overall exertion level in the exoskeleton operator was relatively low while performing the upstairs exercise.

The distribution between the optimized parameters and D-value of the heart rate variation in uphill terrain is shown in Fig.6. When optimizing the parameters for this terrain, the number of iterations was set to 10. As can be seen from the Fig.6, the body has the smallest change in heart rate when the assistive force parameter is $A = 50$ and $\alpha = -0.051$.

As shown in Fig.7, the assistive force parameters on flat ground walking were optimized after 5 iterations. Similarly, the results showed that as the assistive force increased, the heart rate had a tendency to reduce. The effect of different assistive force parameters on heart rate variability is shown in Fig.7. It can be concluded that the subject with the control parameter ($A = 50$, $\alpha = -0.232$) can achieve the least change in heart rate, which shows that it can save energy.

In the three terrains above, the 11 red data points on the function distribution plot corresponding to the collected heart rate dataset in the left panel are the original collected heart rate sampling points. The corresponding red data points on the acquisition function distribution plot in the right panel are the data points corresponding to the optimal parameters.

III. Overall Control Strategy

The overall process on multi-terrains assistive force of the soft exoskeleton is shown in Fig.8. The whole process can be divided into two parts: terrain recognition and assistive force parameter optimization. For terrain recognition, the data (Angle, angular velocity, angular acceleration) is obtained on human walking in different types of terrains. The collected

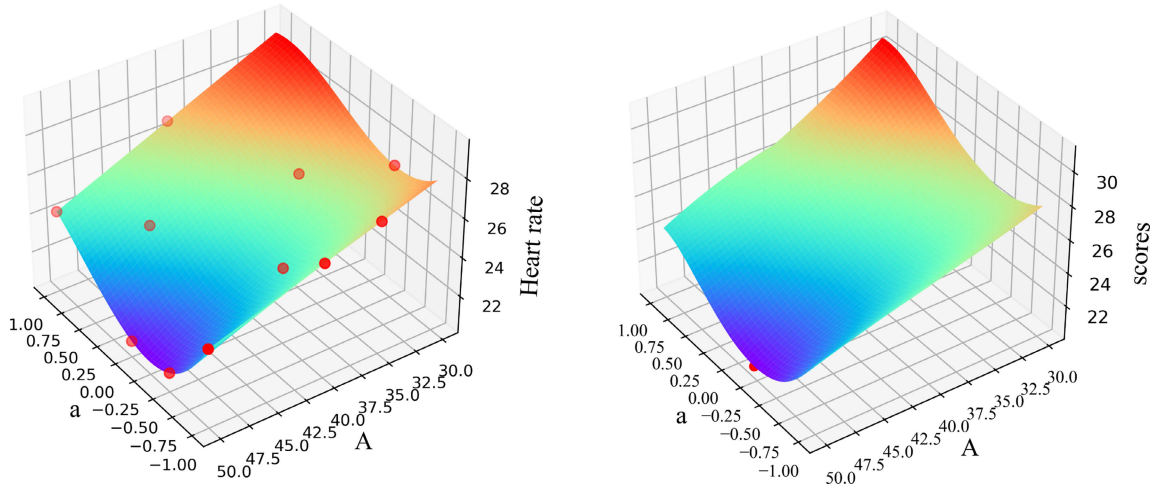

Fig. 7. Parameter optimization results of the flat ground walking mode.

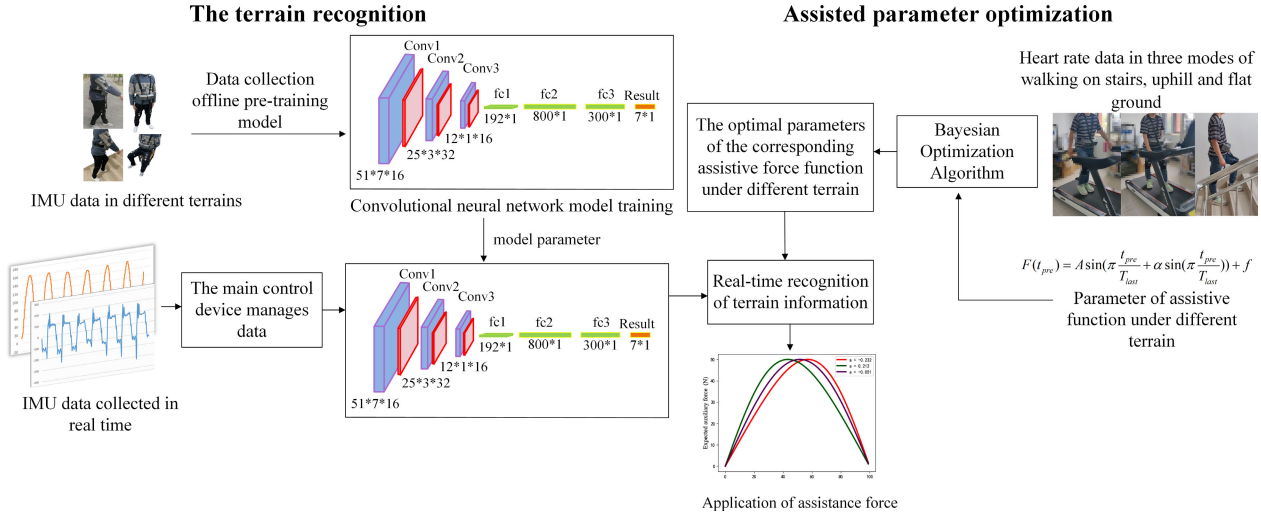

Fig. 8. The process on terrain recognition and the assistive force parameters optimization.

data is filtered to become stable by band-pass filtering and Kalman filtering. Then, the data is transferred to the convolutional neural network (CNN) to train the recognition model offline. The backbone of this convolutional neural network consists of three blocks. Each block consists of a convolutional layer and a pooling layer. The features generated from the backbone are transferred to three fully connected layers to obtain the final result. The pre-trained model was then used for online terrain recognition The recognition experimental results are shown in Fig.9. The online gait recognition method can effectively recognize the different terrain environments. The assistive force parameters A and α corresponding the terrain can be optimized iteratively by the collected D-value on heart rate variation with the Bayesian optimization algorithm.

In the process of walking with soft exoskeleton, the IMU data is real-time collected for terrain identification. When the current terrain is identified as downstairs or downhill, the exoskeleton will not provide assistive force for safety and stability. The downstairs and downhill is the process on potential energy falling of the body's center. It should maintain the stability of the body. When the terrain is identified as flat, the master control device will set $A = 50$, $\alpha = -0.232$ as the parameters of the assistive force equation. When

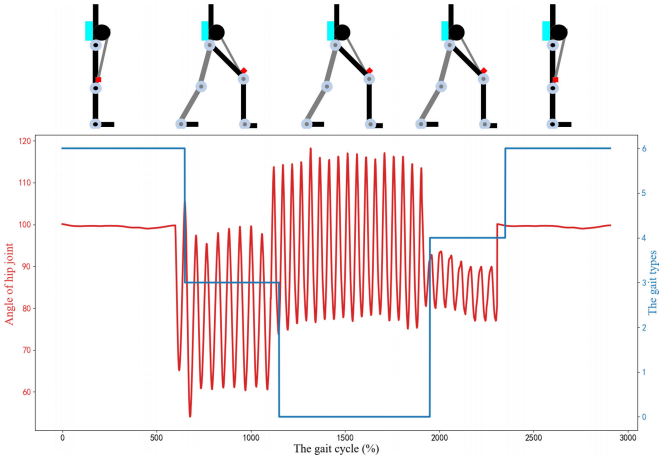

Fig. 9. Terrain recognition results, the red curve is the angle change data of unilateral hip joint, and the blue curve is the recognized gait type. flat ground walking:0, ramp ascent:1, ramp descent:2, stairs ascent:3, stairs descent:4, sitting:5, standing:6.

the terrain is detected as uphill, the master control device will set $A = 50$ and $\alpha = -0.051$ as the control parameters. When the current terrain is detected as upstairs, the master control device will set $A = 50$ and $\alpha = 0.212$ as the parameters.

TABLE II
COMPARISON WITH OTHER PAPERS

Author	Assistance	Weight	Terrain	Others	Metabolic rate reduction
Chunjie Chen[11]	Hip flexion and extension, Knee extension	4.6KG	Slopes (-10°,0°,10°)	NA	9.8%/12.48%/22.08%
Sangjun Lee[26]	Hip flexion and extension, Ankle plantarflexion	5.1KG	Outdoor	NA	16.93%
Qiang Chen [4]	Hip flexion and extension	NA	Slopes (5°)	15kg load	8.53%
Ye Ding[28]	Hip extension	0.859KG	Level ground	NA	17.4 %
Our work	Hip extension	2.3KG	flat terrain, uphill, up stairs	NA	19.6%/11.6%/12.7%

Fig. 10. Metabolic testing experiments in different terrains.

With the above consideration, the assistive force effect can be optimized adaptively. In the next section, we will further verify the effectiveness of the proposed assistive force strategy by metabolic testing.

IV. EXPERIMENTAL VERIFICATION

A. Metabolic Testing

In order to evaluate and validate the effectiveness of our proposed multi-terrains assistive force parameter optimization method, we conducted metabolic experiments on three healthy subjects with different assistive force parameters. The subjects were three male students, 174 ± 6 cm in height and 24±2 years old. They were free of any physical or psychological disorders. In the meanwhile, an informed consent was signed all before the experiment. The experimental procedure is shown in Fig. 10.

The experimental protocol was divided into one day of training and three days of testing. On the day of training, the three subjects were asked to take turns walking for ten minutes on three different terrains wearing our soft exoskeleton equipment and a portable gas analysis system (K4b^2, C, Roma, Italy). The subsequent part of the test was divided into three days, with each person being tested on only one kind of terrain each day. For flat and uphill terrain, the experiment was operated on the treadmill. For upstairs terrain, the experiment was operated on a seven-story laboratory building. The experimental process is shown in Fig.11.

In the test, we used K4b^2 to collect data on oxygen consumption and carbon dioxide emissions from the subjects [23] and then calculated metabolic rates [24], [25]. The net metabolic rate was obtained by subtracting the resting metabolic rate from the metabolic rate under exercise and normalizing it by the subject's body weight.

The net metabolic rates of the subjects with different assistive force parameters on flat ground terrain are shown in Fig.12. Different assistive force parameters produce different effects on different people. Significantly, the net metabolic

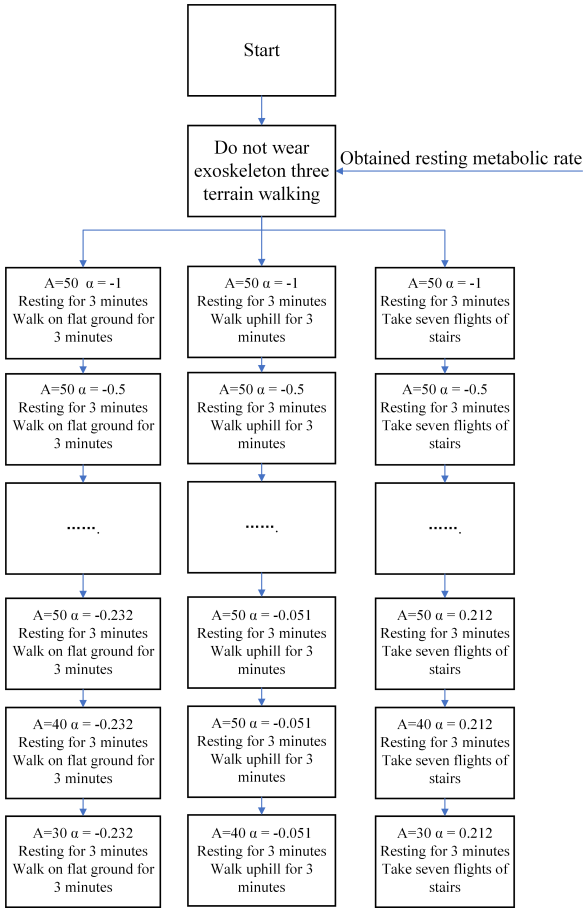

Fig. 11. Experimental flow chart.

rates of all subjects with the optimal assistive force parameters are lower. Compared without assistive force on the metabolic rates, the net metabolic rates were decreased by 12.2%, 22.7%, and 23.9%, respectively, in the three subjects with optimal exoskeleton assistive force parameters.

The net metabolic rates of the subjects with different assistive force parameters on uphill terrain are shown in Fig13. Compared without assistive force on the metabolic rates, the net metabolic rates were decreased by 18.2%, 11.5% and 5.2%, respectively. The net metabolic rates of the subjects with different assistive force parameters on walking upstairs are shown in Fig.14. The net metabolic rates were decreased by 9.7%, 13.2%, and 15.2%, respectively.

B. Comparison and Discussion

Currently, the environment perception is very important for the adaptive control of the exoskeletons. As the method

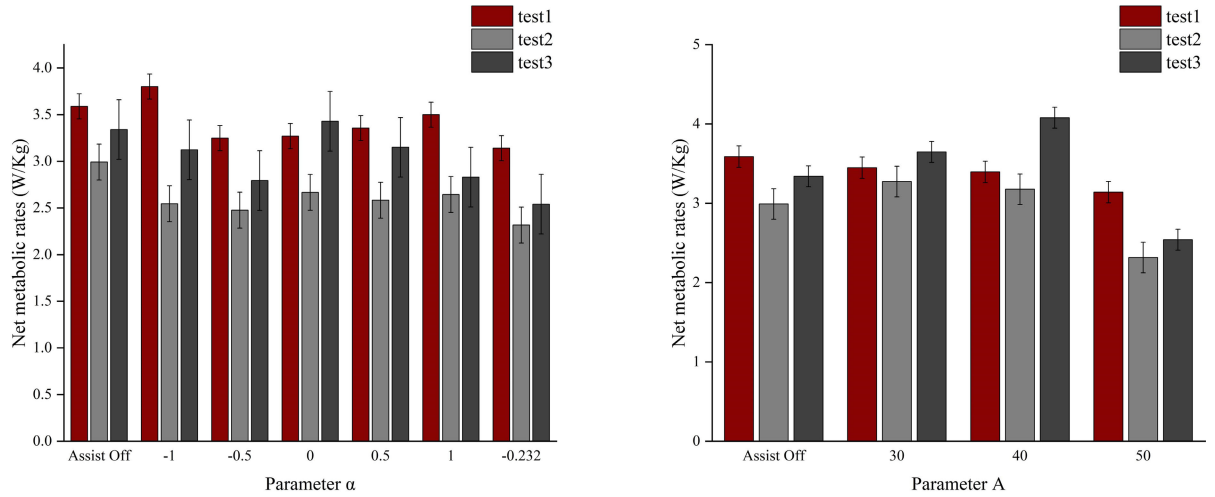

Fig. 12. Net metabolic rate in subjects with different assistive force parameters on the flat ground terrain.

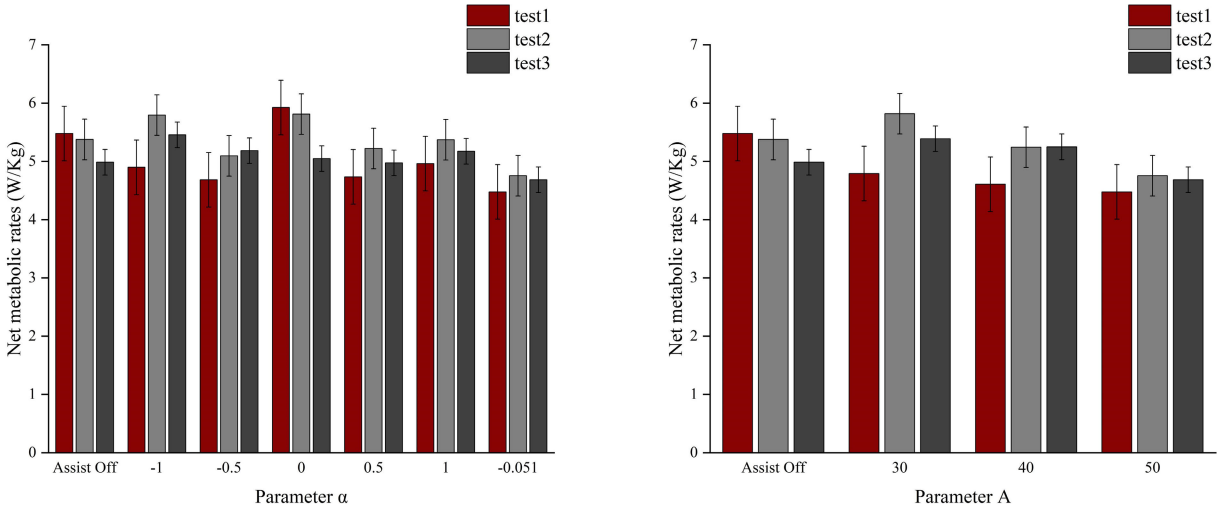

Fig. 13. Net metabolic rate in subjects with different assistive force parameters on uphill terrain.

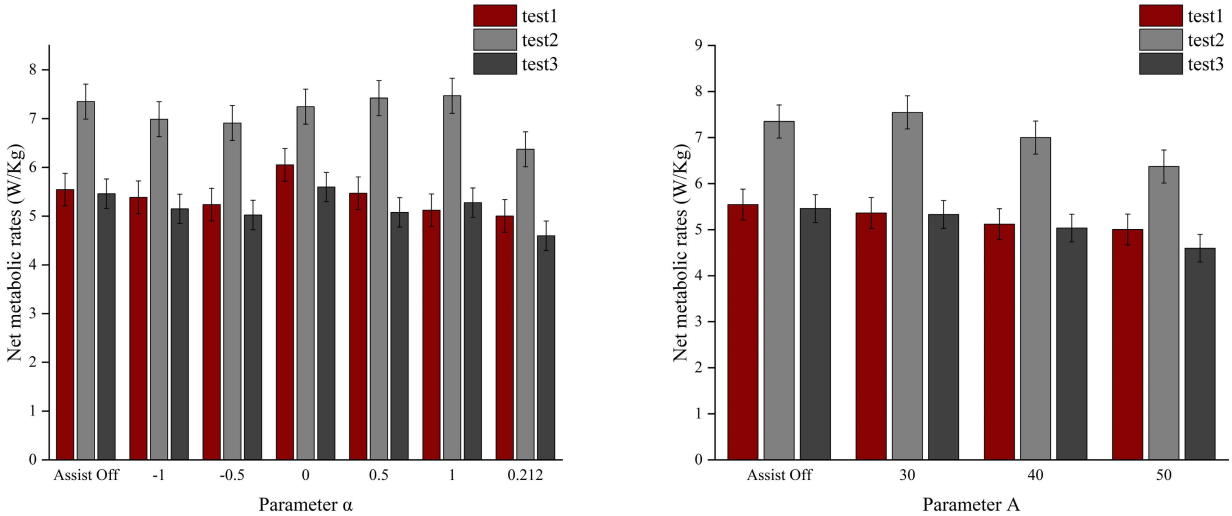

Fig. 14. Net metabolic rate in subjects with different assistive force parameters on the up-stairs terrain.

of the environment perception, deep learning, such as CNN, appears competing performance for multi-terrains recognition. However, it is challenging to control the exoskeletons under different terrains adaptively. To this end, a parameter adaptive optimization method for exoskeleton assist is proposed with multi-terrain. The method is optimized by the Bayesian optimizer to calculate the optimal assistive parameters for three types of terrains: uphill, downhill and flat. With this consideration, the soft exoskeleton can adapt to different terrain environments effectively.

There are also many studies in the literature about exoskeletons with different assistive terms. Some of which are shown in TABLE II. By comparison, our exoskeleton equipment is not only lighter in weight, but also can be adapted to different terrain environments. In the meanwhile, the proposed adaptive control method can save more energy consumption in several common types of terrain. As shown in the TABLE II, the exoskeleton proposed by Chen et al. [11] reduced metabolic value by 22.08% in the uphill environment. We considered that the hip flexion extension and knee synergistic assistive solution would be more effective than our hip extension assist. In addition, the exoskeleton proposed by Ding et al. [27] had a lighter weight with the same hip extension assistive force. Compared with his work, the efficiency of assistive force about our work was more competitive.

V. Conclusion

The aim of this study is to develop a hip-assisted soft exoskeleton that can be adapted to different terrains. This will help exoskeleton wearers in their daily activities and provide them with better walking support. Therefore, we propose a method to optimize the assistive force parameters based on a Bayesian optimization algorithm. The assistive force parameters A and α are optimized by the Bayesian optimization algorithm. Meanwhile, the heart rate variations for different terrains are collected as the dataset to generate the optimal parameters. Finally, the metabolic is conducted on three subjects. The results show that the average net metabolic rate of the subjects decreased by 19.6% on flat ground, 12.7% on upstairs, and 11.6% uphill. The above experimental results verified the effectiveness of the proposed multi-terrain assistive force method. In the future, we will combine soft exoskeletons with reinforcement learning so that our devices can adapt to more complex road conditions in real-life environments and generate different assistive parameters based on different wearers' characteristics.

References

[1] D. Shi, W. Zhang, W. Zhang, and X. Ding, "A review on lower limb rehabilitation exoskeleton robots," *Chin. J. Mech. Eng.*, vol. 32, no. 1, pp. 1–11, Dec. 2019.

[2] H. Lee, W. Kim, C. Han, and J. Han, "The technical trend of the exoskeleton robot system for human power assistance," *Int. J. Precis. Eng. Manuf.*, vol. 13, no. 8, pp. 1491–1497, 2012.

[3] A. J. Young and D. P. Ferris, "State of the art and future directions for lower limb robotic exoskeletons," *IEEE Trans. Neural Syst. Rehabil. Eng.*, vol. 25, no. 2, pp. 171–182, Feb. 2017.

[4] Q. Chen, S. Guo, L. Sun, Q. Liu, and S. Jin, "Inertial measurement unit-based optimization control of a soft exosuit for hip extension and flexion assistance," *J. Mech. Robot.*, vol. 13, no. 2, Apr. 2021, Art. no. 021016.

[5] S. V. Sarkisian, M. K. Ishmael, and T. Lenzi, "Self-aligning mechanism improves comfort and performance with a powered knee exoskeleton," *IEEE Trans. Neural Syst. Rehabil. Eng.*, vol. 29, pp. 629–640, 2021, doi: 10.1109/TNSRE.2021.3064463.

[6] D.-H. Lim, W.-S. Kim, H.-J. Kim, and C.-S. Han, "Development of real-time gait phase detection system for a lower extremity exoskeleton robot," *Int. J. Precis. Eng. Manuf.*, vol. 18, pp. 681–687, May 2017.

[7] L. Xing, M. Wang, J. Zhang, X. Chen, and X. Ye, "A survey on flexible exoskeleton robot," in *Proc. IEEE 4th Inf. Technol., Netw., Electron. Autom. Control Conf. (ITNEC)*, Jun. 2020, pp. 170–174.

[8] S. Ding, X. Ouyang, T. Liu, Z. Li, and H. Yang, "Gait event detection of a lower extremity exoskeleton robot by an intelligent IMU," *IEEE Sensors J.*, vol. 18, no. 23, pp. 9728–9735, Dec. 2018.

[9] O. Ulkir, G. Akgun, A. Nasab, and E. Kaplanoglu, "Data-driven predictive control of a pneumatic ankle foot orthosis," *Adv. Electr. Comput. Eng.*, vol. 21, no. 1, pp. 65–74, 2021.

[10] L. Ma, Y. Leng, W. Jiang, Y. Qian, and C. Fu, "Design an underactuated soft exoskeleton to sequentially provide knee extension and ankle plantarflexion assistance," *IEEE Robot. Autom. Lett.*, vol. 7, no. 1, pp. 271–278, Jan. 2022.

[11] C. Chen et al., "Iterative learning control for a soft exoskeleton with hip and knee joint assistance," *Sensors*, vol. 20, no. 15, p. 4333, Aug. 2020.

[12] H. Liu, J. Tao, P. Lyu, and F. Tian, "Human–robot cooperative control based on sEMG for the upper limb exoskeleton robot," *Robot. Auto. Syst.*, vol. 125, Mar. 2020, Art. no. 103350.

[13] Q. Zhang et al., "Imposing healthy hip motion pattern and range by exoskeleton control for individualized assistance," *IEEE Robot. Autom. Lett.*, vol. 7, no. 4, pp. 11126–11133, Oct. 2022.

[14] D. F. N. Gordon, T. Matsubara, T. Noda, T. Teramae, J. Morimoto, and S. Vijayakumar, "Bayesian optimisation of exoskeleton design parameters," in *Proc. 7th IEEE Int. Conf. Biomed. Robot. Biomechatronics (Biorob)*, Aug. 2018, pp. 653–658.

[15] A. Shahrokhshahi, M. Khadiv, A. Taherifar, S. Mansouri, E. J. Park, and S. Arzanpour, "Sample-efficient policy adaptation for exoskeletons under variations in the users and the environment," *IEEE Robot. Autom. Lett.*, vol. 7, no. 4, pp. 9020–9027, Oct. 2022.

[16] H. R. Harrison and T. Nettleton, "2—Lagrange's equations," in *Advanced Engineering Dynamics*, H. R. Harrison and T. Nettleton, Eds. London, U.K.: Butterworth-Heinemann, 1997, pp. 21–45.

[17] S. Guo, Q. Xiang, K. Hashimoto, and S. Jin, "Assistive force of a belt-type hip assist suit for lifting the swing leg during walking," in *Proc. IEEE Int. Conf. Robot. Autom. (ICRA)*, Paris, France, May 2020, pp. 4841–4847.

[18] C. Thornton, F. Hutter, H. H. Hoos, and K. Leyton-Brown, "Auto-WEKA: Combined selection and hyperparameter optimization of classification algorithms," in *Proc. 19th ACM SIGKDD Int. Conf. Knowl. Discovery Data Mining*, Chicago IL, USA, Aug. 2013, pp. 847–855.

[19] J. Snoek, H. Larochelle, and R. P. Adams, "Practical Bayesian optimization of machine learning algorithms," in *Proc. Adv. Neural Inf. Processing Syst.*, vol. 29, Aug. 2012, pp. 1–9.

[20] F. Pérez-Cruz, S. Van Vaerenbergh, J. Murillo-Fuentes, M. Lazaro-Gredilla, and I. Santamaria, "Gaussian processes for nonlinear signal processing: An overview of recent advances," *IEEE Signal Process. Mag.*, vol. 30, no. 4, pp. 40–50, Jul. 2013.

[21] C. E. Rasmussen, "Gaussian processes in machine learning," in *Advanced Lectures on Machine Learning*, vol. 3176, O. Bousquet, U. Von Luxburg, and G. Ratsch, Eds. Berlin, Germany: Springer, 2004, pp. 63–71.

[22] N. Srinivas, A. Krause, S. M. Kakade, and M. W. Seeger, "Information-theoretic regret bounds for Gaussian process optimization in the bandit setting," *IEEE Trans. Inf. Theory*, vol. 58, no. 5, pp. 3250–3265, May 2012.

[23] R. Duffield, B. Dawson, H. C. Pinnington, and P. Wong, "Accuracy and reliability of a Cosmed K4b^2 portable gas analysis system," *J. Sci. Med. Sport*, vol. 7, no. 1, pp. 11–22, Mar. 2004.

[24] D. R. Westenskow et al., "Calculation of metabolic expenditure and substrate utilization from gas exchange measurements," *J. Parenteral Enteral Nutrition*, vol. 12, no. 1, pp. 20–24, Jan. 1988.

[25] S. Galle, P. Malcolm, S. H. Collins, and D. De Clercq, "Reducing the metabolic cost of walking with an ankle exoskeleton: Interaction between actuation timing and power," *J. Neuroeng. Rehabil.*, vol. 14, p. 35, Apr. 2017.

[26] S. Lee et al., "Autonomous multi-joint soft exosuit for assistance with walking overground," in *Proc. IEEE Int. Conf. Robot. Autom.*, Brisbane, QLD, Australia, May 2018, pp. 2812–2819.

[27] Y. Ding, M. Kim, S. Kuindersma, and C. J. Walsh, "Human-in-the-loop optimization of hip assistance with a soft exosuit during walking," *Sci. Robot.*, vol. 3, no. 15, Feb. 2018, Art. no. eaar5438.